Published in
14th International School on Quantum Electronics: Laser Physics and Applications 6604, issue 66040L, 1-5, 2007
which should be used for any reference to this work

Sub-Doppler diode laser frequency stabilization with the DAVLL scheme on the D_1 line of a ^{87}Rb vapor-cell

R. Giannini[2,(a)], E. Breschi[1], C. Affolderbach[1], G. Bison[3], G. Mileti[1], H. P. Herzig[2], A. Weis[3]

[1] Observatoire cantonal de Neuchâtel, Rue de l'Observatoire 58, 2000 Neuchâtel, Switzerland
[2] Institute of Microtechnology, University of Neuchâtel, A.-L. Breguet, 2000 Neuchâtel, Switzerland
[3] Departement of Physics, University of Fribourg, Chemin du Musée 3, 1700 Fribourg, Switzerland

ABSTRACT

We established an experimental set-up that allows laser stabilization using the Doppler[1] and sub-Doppler[2,3] Dichroic Atomic Vapor Laser Locking (DAVLL) and the Saturated Absorption (SA) scheme. In this report we present comparative studies between Doppler and sub-Doppler DAVLL using heterodyne frequency stability measurements with an independently SA stabilized laser. Some major sources of frequency instability are discussed together with ways to improve the stability. Special focus is laid on the sub-Doppler DAVLL stabilization technique where a new approach for getting higher stability is introduced. In our measurements, the ^{87}Rb D_1 line was used as reference atomic line.

Keywords: frequency stabilization, DAVLL, Doppler-free DAVLL, Rubidium

1. INTRODUCTION

Frequency stabilized laser sources are widely used in atomic physics experiments such as laser spectroscopy, laser cooling and trapping. They are also an important component in different applications, for instance in atomic magnetometers, optical interferometers and atomic clocks.

A laser stabilization technique is characterized by its way to generate an error signal. The curve of a typical error signal consists of a zero-crossing at the desired laser emission frequency with a steep slope around it. The slope guarantees a fast reaction to the fluctuations of the central emission frequency. Most stabilization techniques need a modulation (e.g. of the laser current or of an additional electric or magnetic field) and a subsequent lock-in detection to generate this signal. By contrast, DAVLL techniques are not based on any modulation but on the difference of two suitable absorption spectra. This leads to a reduction of the electrical part of the set-up and to a different dependency of a DAVLL stabilized laser on environmental and operational parameter.

An additional advantage of DAVLL is its possibility to tune the stabilized laser over a range of some hundreds of MHz by introducing an offset between the two absorption spectra needed for DAVLL[4].

2. METHOD

The DAVLL technique exploits differences in the absorption spectra of left and right circularly polarized light (σ^-, σ^+) in an atomic system. The atomic sample, in our case ^{87}Rb, is contained in a sealed cell. The Zeeman levels of the atoms are separated in energy by applying a magnetic field over this cell. In fig 1a, the light-atom interaction scheme for the hyperfine transitions starting from F = 2 to F' = 1 is shown for the ^{87}Rb D1 line. The observed absorption spectra for polarized light is the superposition of the absorption lines of the possible transitions between single Zeeman levels (according to the selection rules). This leads to shifted spectra for left and right circularly polarized light. The DAVLL error signal is generated by building the difference of these two spectra, fig. 1b.

If a pump-probe configuration is established, sub-Doppler dips appear in the σ^-, σ^+ absorption spectra[3]. The difference of these two sub-Doppler absorption spectra shows an additional zero crossing with a clearly steeper slope but smaller

(a) E-mail: reto.giannini@unine.ch

capture range and reduced tuning range, fig. 1b,c. Stabilization of a laser using this steeper slope leads to the so-called sub-Doppler DAVLL.

The stability in time of an actively stabilized laser is calculated by the use of the Allan Variation. A more descriptive model for estimating the short-term stability is given by ref. 5. Hence, the short-term stability is determined by the detection noise N, the transition frequency ν_0 and the characteristic of the error signal, i.e. the signal strength S and its width $\Delta\nu$ (or the discriminator slope $D \approx S/\Delta\nu$):

$$\sigma_y(\tau) \approx \frac{\Delta\nu}{\nu_0} \cdot \frac{0.2}{S/N} \cdot \tau^{-1/2} \qquad (1)$$

This model of short-term stability shows two ways to improve a set-up: first, reduction of $\Delta\nu/\nu_0$ (i.e. enhancement of the Q-factor) and second, optimization of the S/N ratio, see section 4.

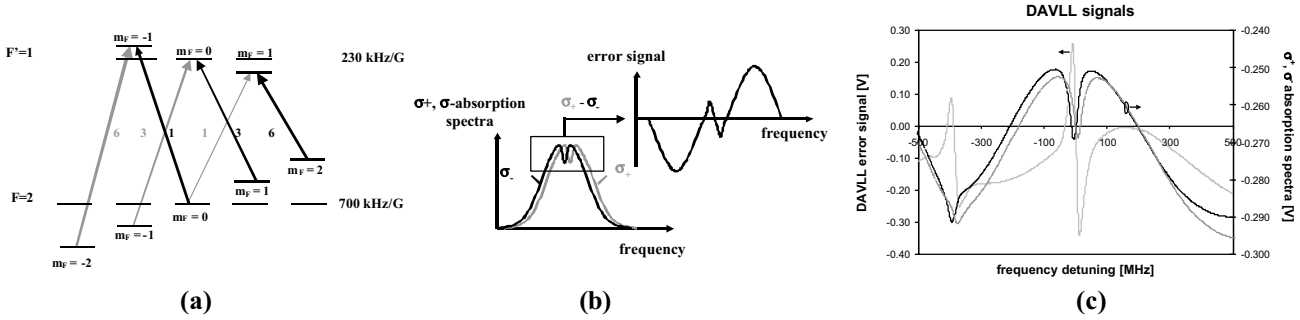

Fig. 1: (a) Energy levels of the ^{87}Rb D_1, F = 2, F' = 1 transition. The arrows indicate the possible transitions for left (black) and right (grey) circularly polarized light. The numbers next to the arrows are the relative transition probabilities. The number on the right shows the splitting of the Zeeman levels by a magnetic field.
(b) Generation of a sub-Doppler DAVLL error signal by building the difference of the absorption spectra of left (σ^-) and right (σ^+) circularly polarized light.
(c) Experimentally observed sub-Doppler DAVLL signals.

3. EXPERIMENTAL SET-UP

In order to study Doppler and sub-Doppler DAVLL with respect to SA, the set-up is based on the use of two lasers that can be independently stabilized. One laser can be stabilized using the SA technique and the other using sub-Doppler or Doppler DAVLL, fig 2. In both arms of the set-up, a home-made Extended Cavity Diode Laser[6] (ECDL) emitting at 795 nm (^{87}Rb D_1-line) with a line width of ~300 kHz was stabilized. An additional SA system in the DAVLL part can be used to verify that the stability of the SA stabilized laser is better than the DAVLL stabilized laser, i.e. the observed stability out of the heterodyne frequency measurement is limited by DAVLL. The set-up gives the possibility to vary the most important environmental and operating parameters.

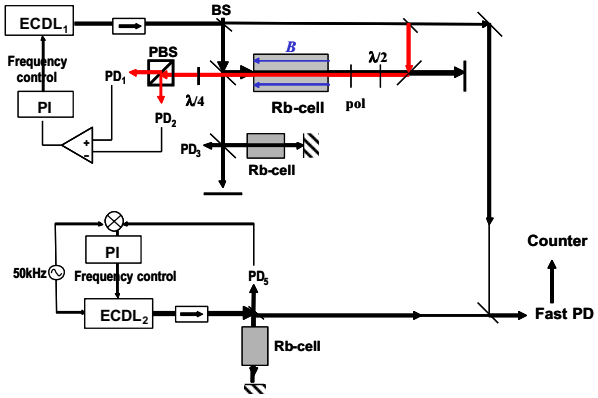

Fig. 2: used set-up for comparative studies and analysis of sources of instabilities.
ECDL: Extended Cavity Diode Laser, (P)BS: (Polarizing) Beam Splitter, PD: Photo Diode, PI: Proportional plus Integral controller, Pol: Polarizer

In the DAVLL arm, a 5 cm long, evacuated reference cell containing Rb in natural isotope mixture is used. The cell is placed between two toric magnets that generate a magnetic field strength of ~10 G. The surrounding cylinder is designed to minimize stray magnetic fields[7]. During the experiments, the cell temperature was 35°C. Sub-Doppler DAVLL stabilization is performed by splitting the emitted light and creating a pump-probe configuration. The maximal pump beam intensity is around 8.4 mW/cm^2 (beam diameter 2.4 mm) and the maximal probe beam intensity is 8.0 mW/cm^2 (beam diameter 1.2 mm). Intensity and polarization of pump and probe beam can independently be changed. For Doppler DAVLL experiments, the pump beam is blocked using a shutter. The DAVLL error signal is generated by building the difference of the two PD-signals of a circular analyzer[4].
The vapor cell in the SA arm is shielded against magnetic fields and can be heated up to 70°C. For a more detailed description of the used SA system see ref. 9.

4. EXPERIMENTAL RESULTS

In a first step, we focused on optimization of the set-up to reach a better short-term stability. This was done by improving the signal S and reducing the noise N. The optimal values of short-term stability in our set-up estimated by using equation (1) are:

DAVLL: $\sigma_y(\tau = 1s) = 4 \cdot 10^{-10}$
Sub-Doppler DAVLL: $\sigma_y(\tau = 1s) = 9 \cdot 10^{-12}$
SA: $\sigma_y(\tau = 1s) = 5 \cdot 10^{-12}$

The SA value is added to show that the heterodyne frequency stability measurements are still dominated by instabilities of the DAVLL stabilized laser. However, one can notice that the sub-Doppler DAVLL gets comparable to the SA stabilized laser. A further improvement, especially of the sub-Doppler DAVLL, seems possible by reduction of the line width $\Delta\nu$ that is still dominated by power broadening.
Fig. 3 shows two examples of the behavior in time of the beat signal between a sub-Doppler DAVLL and a SA stabilized laser. The slope in both figures is due to a temperature driven change of the position of the zero-crossing of the error signal in the sub-Doppler DAVLL system. The clearly visible oscillation in fig. 3b can be explained by etalon effect due to a cavity of ~5 cm (i.e. the cell in the DAVLL system). The influence of etalon effect was successfully reduced by optimizing the set-up, as can be seen by comparing fig. 3a and 3b. One can remark that a smaller oscillation is present in both plots. This oscillation is still under investigation to obtain a further improvement of the stability.
Out of beat signal measurements as shown in fig. 3, the stability of a (sub-) Doppler DAVLL stabilized laser was estimated by calculating Allan Deviation. Fig. 4 shows the Allan Deviation of a DAVLL (fig. 4a) and a sub-Doppler DAVLL (fig. 4b) stabilized lasers. The theoretical estimations using equation (1) are added in both cases. Theoretical and experimental values are in good accordance. The difference in stability between DAVLL and sub-Doppler DAVLL is due to a much broader error signal in the case of DAVLL ($\Delta\nu$ = 360 MHz compared to $\Delta\nu$ = 21 MHz in the case of sub-Doppler DAVLL). The error signal strength S is comparable in both cases.
The width $\Delta\nu$ of the error signal is not only in direct relation to the stability but to the tuning range of a stabilized laser, too. Thus, the tuning range of the DAVLL stabilized laser is much bigger than the one of the sub-Doppler stabilized laser. The tuning itself can be achieved by adding optically or electronically an offset[4].

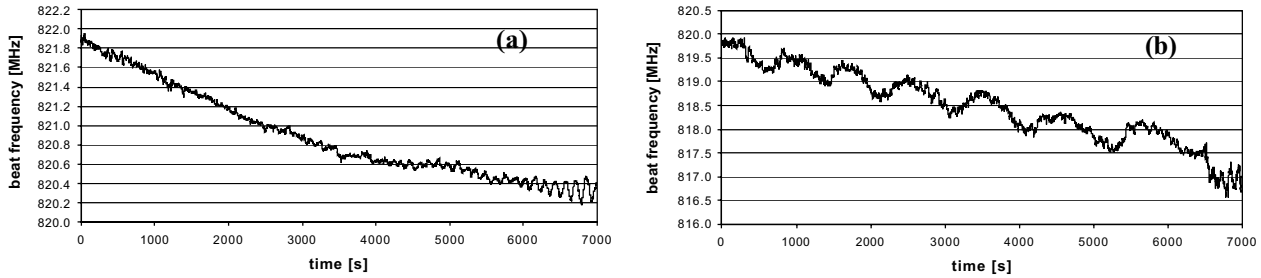

Fig. 3: Beat signal between a sub-Doppler DAVLL and a SA stabilized laser. (a) after optimization, (b) with a set-up that is influenced by etalon effect.

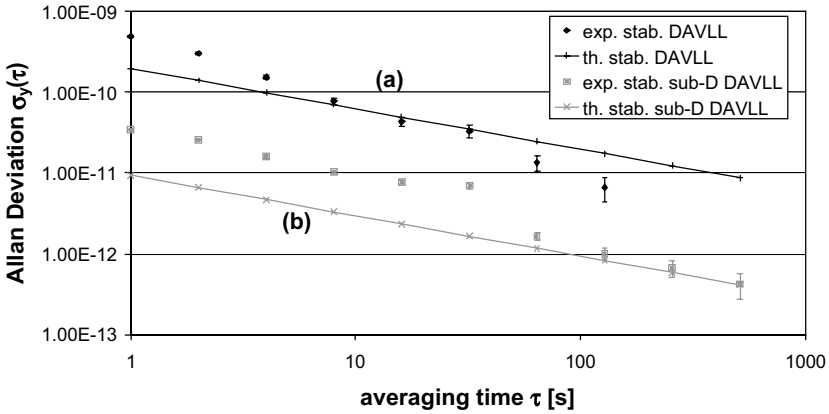

Fig. 4: Experimental and theoretical stability of a laser locked with (a) DAVLL, (b) sub-Doppler DAVLL to the ^{87}Rb D1 line.

A more precise analysis of the physical processes in a sub-Doppler DAVLL system leads to other possibilities of further improvement of the stability. The most important physical process within the DAVLL cell is for our purpose the interaction of intense polarized light with atoms influenced by a magnetic field in the linear Zeeman regime. The intense polarized light leads to optical pumping. For getting a general idea of the influence of the magnetic field, a suitable choice of the quantization axis **QA** is essential. If **QA** is chosen parallel to the magnetic field **B**, the Zeeman levels $|m_F>$ are eigenstates of the Hamiltonian H_{Zeeman}. In an idealized situation for DAVLL stabilization as shown in fig. 5a, **QA** $\parallel$ **B** means **QA** $\perp$ **E**, too, where **E** describes the direction of the electric field of the light beams. Thus, for the light-atom interaction linearly polarized light within a plane perpendicular to **k** has to be seen as a superposition of left and right circularly polarized light, σ^{+-}. For a more detailed description see e.g. ref. 8.

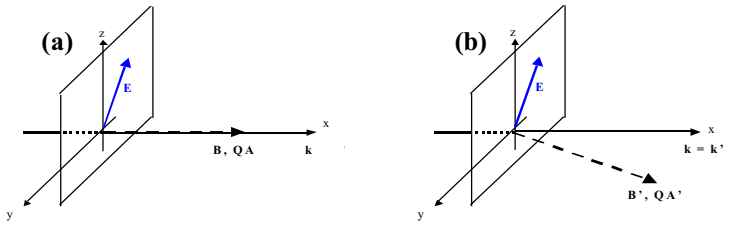

Fig. 5: Choice of quantization axis **QA**, beam propagation direction **k** and polarization **E** in the two discussed systems: (a) idealized DAVLL system with **E** $\perp$ **B**. (b) System with an **E** field component $\parallel$ to **B**.

If the magnetic field **B'** has a not negligible component perpendicular to **k** (= **k'**), the light-atom interaction alters. By taking the quantization axis **QA'** parallel to **B'** again, the light beam obtains a polarization component parallel to **QA'**, fig. 5b. This leads to an additional contribution of linear polarized light (π) in the light-atom interaction and therefore to transitions between Zeeman levels characterized by $\Delta m_F = 0$, fig. 1a. The strength of this contribution is dependent on the orientation of **E** relative to **QA'**. This **E**-dependent relative parts of σ^-, σ^+ and π in the light-atom interaction leads to changed optical pumping that becomes manifest in the sub-Doppler absorption spectra.

A physical situation as described can most easily be observed by changing the polarization direction of pump and probe beam within a plane perpendicular to **k**. Fig. 6 shows the PD signals of a circular analyzer for a probe beam polarization perpendicular (fig. 6a) and parallel (fig. 6b) to the test bench. A change of the sub-Doppler dip characteristic is clearly visible for the 21' transition whereas the 22' transition is only slightly influenced by the direction of **E**. Reversed SA-peaks at the 21' transition can be observed with the used set-up.

The 21' absorption spectra for each PD can be fitted using the superposition of a Gaussian (G1, for the Doppler broadened part) and two shifted Lorentzian curves (L2, L3) with opposite signs. Fig. 7 shows the amplitude of L3 relative to the Doppler-broadened peak amplitude. The pump beam polarization was fixed perpendicular to the test bench during this measurement.

The benefit out of these considerations is the possibility to improve the stability of the sub-Doppler DAVLL stabilized laser by optimizing the polarization of pump and probe beam, the magnetic field strength parallel and perpendicular to **k** and the beam intensities. First analysis show that already the optimization of the polarization in our set-up leads to an enhancement of the signal S by a factor two. This is due to the fact that there are polarization directions that show a sub-

Doppler peak in the signal of one PD and a dip in the other at the same time, fig. 6. It is expected that an optimization of all three parameters will lead to a clearly better stability.

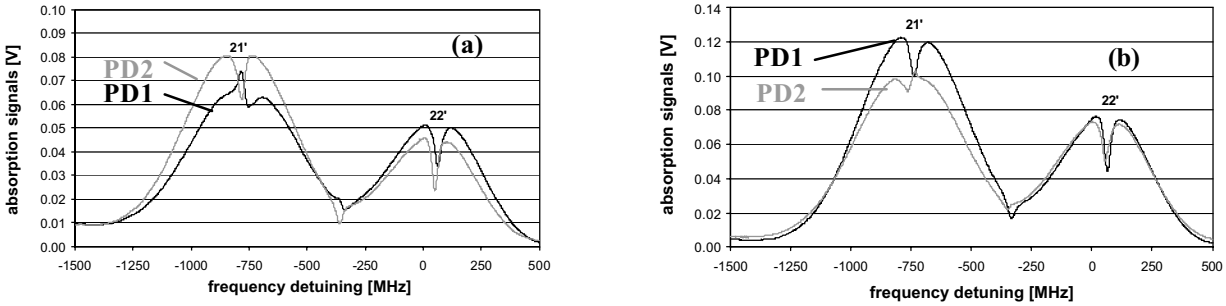

Fig. 6: PD signals of a circular analyzer, (a) probe beam polarization perpendicular to the test bench, (b) probe beam polarization parallel to the test bench.

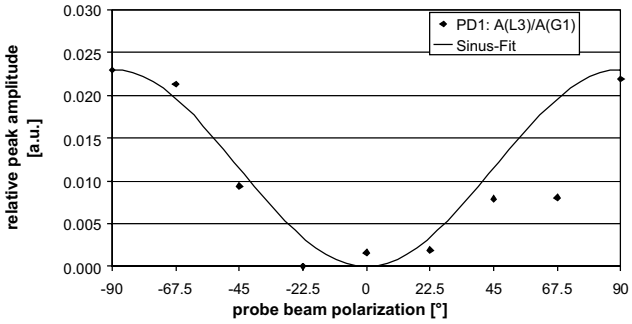

Fig. 7: Polarization dependent amplitude of L3 relative to G1 amplitude for PD1 (see text).

We have improved the stability of a sub-Doppler DAVLL stabilized laser up to an experimentally observed short-term stability of $3 \cdot 10^{-11}$ at $\tau = 1$s and compared it with the stability of a Doppler broadened DAVLL stabilized laser. Examples of influences on the medium and long-term stability are given (Etalon Effect, temperature drift). Additionally, an alternative approach for a further improvement based on optical pumping has been introduced.

REFERENCES

1. K. L. Corwin, Zheng-Tian Lu, C. F. Hand, R. J. Epstein, W. E. Wieman, "Frequency-stabilized diode laser with the Zeeman shift in an atomic vapor", App. Opt. 37, 3295 (1998)
2. T. Petelski, M. Fattori, G. Lamporesi, J. Stuhler, G. M. Tino, "Doppler-free spectroscopy using magnetically induced dichroism of atomic vapor: a new scheme for laser frequency locking", Eur. Phys. J. D 22, 279 (2003)
3. G. Wasik, W. Gawlik, J. Zachorowski, W. Zawadzki, "Laser frequency stabilization by Doppler-free magnetic dichroism", Appl Phys. B, 613 (2002)
4. V. V. Yashckuk, D. Budker, J. R, Davis, "Laser frequency stabilization using linear magneto-optics", Rev. of Sc. Inst., 341 (2000)
5. J. Vanier, L.-G. Bernier, "On the signal-to-noise ratio and short-term stability of passive Rubidium frequency standards", IEEE Transactions on Instrumentation and Measurement, IM-30, 4, 277 (1981)
6. C. Affolderbach, G. Mileti, "Tunable, stabilized diode lasers for compact atomic frequency standards and precision wavelength references", Optics and Lasers in Engineering 43, 291 (2005)
7. S. Marenbach, D. Meschede, internal publication (2001)
8. O. Schmidt, K. M. Knaak, R. Wynands, D. Meschede, "Cesium saturation spectroscopy revisited: How to reverse peaks and observe narrow resonances", Appl. Phys. B 59, 167 (1994)
9. C. Affolderbach, G. Mileti, D. Slavov, C. Andreeva, S. Cartaleva, "Comparison of simple and compact "Doppler" and "sub-Doppler" laser frequency stabilization schemes", Proceedings of the 18th EFTF (2004)